applied sciences

MDPI

Article

Adaptive Optimization Method for Piled Raft Foundations Based on Variable Pile Spacing

Chenyang Yuan [1,*], Yunfei Xie [2,*] and Mang Ou [3]

[1] School of Water Conservancy, North China University of Water Resources and Electric Power, Zhengzhou 450046, China
[2] School of Architecture, North China University of Water Resources and Electric Power, Zhengzhou 450046, China
[3] School of Architecture Engineering, Zhengzhou University of Industrial Technology, Zhengzhou 450046, China
* Correspondence: yuanchenyang@ncwu.edu.cn (C.Y.); yf_xie_yzr@163.com (Y.X.)

Abstract: Stricter control of the differential settlement is always required in important buildings more than in ordinary buildings. It becomes a necessity to find a simple and efficient optimum design method for pile foundations in terms of performance and economy. In this paper, an adaptive optimization method (AOM) is proposed to reduce the differential settlement of the pile group and piled raft, in which the piles are located in appropriate locations according to the settlement characteristic of the raft. Piled raft foundations with different types of load and different raft shapes are optimized using this method; soil inhomogeneity and nonlinear characteristic are considered during this process. The optimization results show that the reductions of the differential settlement are more than 80%. The overall foundation performances are improved as the maximum settlements of the foundations are reduced. The maximum bearing capacity of the pile group is no more than its ultimate bearing capacity after optimization design, and part of the excess bearing capacity can be translated into economic savings (AOM-ES). By keeping a good optimization effect of the differential settlement, the number of piles can be reduced by AOM-ES compared with the initial design. The AOM is robust and can be applied to the piled foundations of various raft shapes in layered soils under complex vertical loads with no significant impact on optimization efficiency.

Keywords: piled raft foundations; adaptive optimization method; variable pile spacing; differential settlement; economic savings

check for updates

Citation: Yuan, C.; Xie, Y.; Ou, M. Adaptive Optimization Method for Piled Raft Foundations Based on Variable Pile Spacing. *Appl. Sci.* **2023**, *13*, 1648. https://doi.org/10.3390/app13031648

Academic Editor: Daniel Dias

Received: 3 January 2023
Revised: 18 January 2023
Accepted: 24 January 2023
Published: 28 January 2023

Copyright: © 2023 by the authors. Licensee MDPI, Basel, Switzerland. This article is an open access article distributed under the terms and conditions of the Creative Commons Attribution (CC BY) license (https://creativecommons.org/licenses/by/4.0/).

1. Introduction

Pile foundations are preferred for supporting tall buildings and important structures [1–5] (e.g., high-rise buildings, nuclear power plants, and tall wind turbines), because pile foundations are good at controlling the differential and total settlement and improving the bearing capacity. However, the selection of suitable related parameters of pile foundations and the corresponding geotechnical design requires a complex process [6–10]. A larger design load or complex superstructure can always result in a more complex foundation design, e.g., making the foundations larger or more irregular, which will result in more resources being allocated for foundation design and construction to meet safety requirements. The foundation design and construction usually account for a large proportion of the total cost of the building, so it is necessary to improve the economic benefits of the foundation by optimizing the design.

Through a large number of studies, it has been found that the optimal design can reduce the total and differential settlement of the raft, and improve the utilization of the bearing capacity of the pile foundation [11–18]. For the design of large and irregular pile groups, the control of the differential settlement is particularly important [19–21]. To address this issue, Padfield and Sharrock [22] proposed a method intended to enhance

the performance of the pile group by changing the geometries of each pile. Kim et al. [23] determined the optimal pile locations in a piled raft design applying the genetic algorithm. Nguyen [17,18] gave a parametric study for the optimal design of large pile foundations on sand and commented that adding piles in the centre of a raft can reduce the differential settlement effectively. Y.F. Leung et al. [24] proposed an optimization analysis method for the pile foundation, which uses the compression matrix of the bending characteristics of the superstructure to consider the stiffness of the superstructure and the foundation model at the same time. Shrestha et al. [25] introduced a geotechnical design method and its corresponding optimization program for a wind turbine tower pile-raft foundation. This method provides a robust design optimization program based on reliability based on the design parameters under simplified site conditions. Chan et al. [13], Ng et al. [26], Hwang et al. [27], and Liu et al. [28] studied the application of the evolutionary algorithm in basic optimization design.

Previous studies on the optimization of design basis by numerical methods mostly used traditional gradient methods or genetic algorithms, but these methods have certain limitations, such as the requirement that the design problem should be mathematically formulated and differentiable, and the calculation cost is very high (especially for large-scale pile groups). Therefore, it is necessary to propose new methods to change this limitation and give full play to the bearing capacity of pile groups. Xie and Chi [29] proposed a simple optimization method to achieve an optimized design of foundation stiffness to reduce the value of the differential settlement. The optimized design fully mobilizes the bearing capacity of each pile by using different pile diameters and different pile spacing. However, the method can be regarded as a semi-automatic optimization method; the existence of human factors will affect the optimization efficiency, and economic optimization was not considered.

In this study, an adaptive optimization method (AOM) is presented for piled raft foundations (PRFs), which apply each pile in an appropriate location to accommodate the differential settlement of the raft. PRFs with different loads and raft shapes are optimized to verify this method. The nonlinear elasticity and inhomogeneity of the soil properties and soil–raft–pile interaction are considered through three-dimensional (3D) finite element analysis during the analysis. The results show that this method doesn't need a complex algorithm and too many iterations, while the optimization rate of the differential settlement of the raft can reach more than 80%. The application of this method is not limited by the shape of the raft and the distribution characteristics of the upper load. The benefits achieved are reflected in the reduction of the differential settlement and the increase of the overall stiffness (reduction of the maximum raft settlement), and the excess bearing capacity of the piles can also be translated into the reduction of the pile group cost.

2. The Theoretical Basis of AOM

Before introducing AOM, it is necessary to introduce a two-dimensional plane problem first. Figure 1 shows a raft that suffers a non-uniform line load $y = f(x)$. The problem is locating the pile to avoid the imbalanced settlement of the raft when there are N piles under the raft. The area between $y = f(x)$ and x-axis is assumed as A_f, and the raft will keep its balance when the pile is located at the co-ordinate of the centroid of A_f according to the mechanical principles (in Figure 1a). In a similar way, we divide A_f into A_1 and A_2, in which $A_1 = A_2$, and locate two piles at the co-ordinate of the centroid of A_1 and A_2, which can also keep the raft in balance (in Figure 1b). The same can be done when the number of piles is N (in Figure 1c).

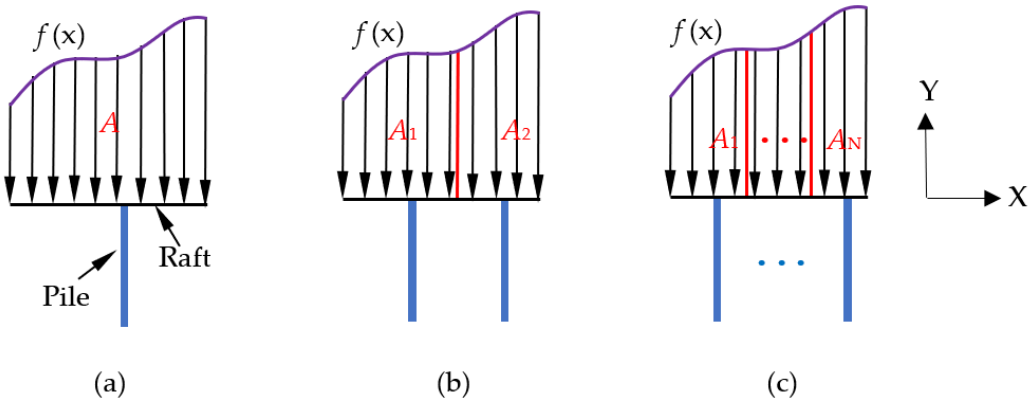


Figure 1. Two-dimensional plane problem of piled raft foundations: (**a**) piled raft with one pile; (**b**) piled raft with two piles; (**c**) piled raft with N piles.

The way to solve the two-dimensional plane problem is also suitable for three-dimensional (3D) space problems. For a 3D problem, the line load changes to the surface load $F = f(x,y)$, and A_f changes to V_T, which is the volume between $f(x,y)$ and co-ordinate axes. We divide V_T into N (N is the number of piles) equal parts, and then the co-ordinate of the centroid of V_i is the location of pile i. Considering that the settlement of the raft is the comprehensive result of the upper load and pile–soil interaction, the settlement distribution of the raft ($z(x,y)$) can be used to replace the distribution of the upper load ($F = f(x,y)$) of the raft in three-dimensional problems. Therefore, V_T can be expressed as

$$V_T = \iint_{A_{raft}} z(x,y)dxdy \tag{1}$$

where A_{raft} is the area of the raft. We divide V_T into N equal parts, and each part is:

$$V_1 = \ldots V_i = \iint_{A_i} z(x,y)dxdy \ldots = V_N \tag{2}$$

where A_i is the projection area of V_i on the co-ordinate axis. The co-ordinate of the centroid of V_i is the location of pile i.

3. Adaptive Optimization Method

There are three main problems during the use of AOM: firstly, determine an initial settlement ($z_0(x,y)$) of the raft; secondly, calculate V_T and divide it into N equal parts; and thirdly, determine the centroid of V_i.

3.1. Determine z_0

Before the optimization design, an initial design is needed to obtain z_0. To reduce the number of iterations during the optimization, a piled raft foundation with the same pile spacing, pile diameter, and pile length designed using the traditional design method is taken as an initial design model. A finite element analysis program, ANSYS, is used to perform the analysis on the piled raft foundation taking the nonlinear behavior of the soil properties and the pile–soil interaction into consideration.

3.2. Calculate V_T and Divide It into Equal Parts

It is difficult to express the settlement surface of the raft using a continuous function (such as $z(x,y)$), and then Equation (1) cannot be used directly. Therefore, a discrete function is adopted instead of the continuous function, using the physical meaning of the integral to solve Equation (1). The settlement surface of the raft is meshed using the interpolation method to form a two-dimensional surface composed of N_t discrete nodes. These nodes

are evenly distributed on the raft surface, assuming each node supports the same size of the raft area, expressed in a_0, in which $a_0 = A_{raft}/N_t$. Then, x, y, and z of each node are represented by matrix [X], [Y], and [Z], where [X] and [Y] represent the x and y co-ordinates of the nodes, and [Z] represents the settlement (z) of the nodes. Finally, Equation (1) can be expressed as

$$V_T = \sum_{j=1}^{N_t} v_j = \sum_{j=1}^{N_t} Z_j \times a_0 \tag{3}$$

where Z_j is the settlement of node j in the matrix [Z], v_j represents the volume supported by point j, and $v_j = Z_j \times a_0$. Equation (2) can be expressed as

$$V_i = V_{avg} = V_T/N, \quad i = 1, 2, 3 \ldots N \tag{4}$$

where V_{avg} represents the average value of N parts.

There are many ways to divide V_T into equal parts. The key is that the shape of V_i needs to be restricted. If the size difference of V_i in the x and y directions is too large, it is easy to cause the centroid spacing of the two adjacent V_i (such as V_i and V_{i+n}) to be too small or even overlapping; that is, the pile spacing is too small or even overlapping, and this does not meet the specification requirements [30]. Therefore, it is necessary to find a search method to limit the shape of V_i in the x and y planes to avoid the situation where the pile spacing is too small or the pile overlap cannot be applied to the actual project.

The central search method (CSM) is applied in AOM to divide V_T. We determine a central point P_i, add v_j of point j (sub-point P_j), which is the nearest to P_i, to v_i continuously, until $v_i + v_1 + v_2 + \ldots + v_j$ is no less than V_{avg} (in Figure 2a). If there are no less than two points with equal distances from P_i, the point with the smallest Z_j has priority. During this process, the central point and its sub-point will be removed from [Z] one after another, and then we go to the next central point. In this way, the sub-points will be spread layer by layer around the central point, which can avoid the issue of the size differences of V_i in the x and y directions being too large. The flow chart of CSM is shown in Figure 2b.

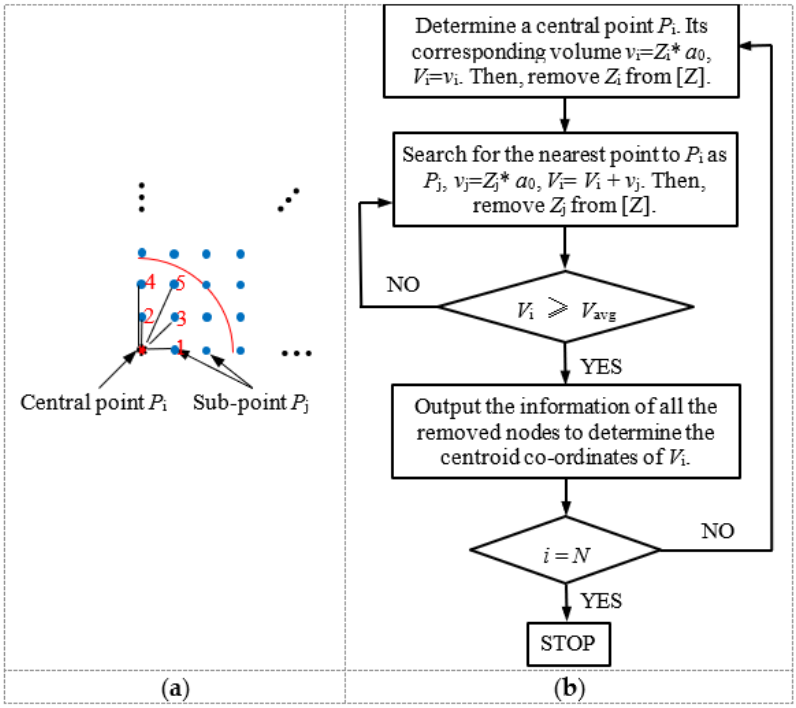


Figure 2. Central search method: (**a**) divide V_T; (**b**) flowchart of CSM .

During the use of CSM, the way to determine a central point is another key point, which can affect the accuracy of search results. For a raft, if the central points are simply determined one by one from one side to the other (for example, from top to bottom, or from left to right), it is easy to leave some points with a large dispersion, or even discontinuous points (call them "leftover material", as shown in Figure 3) along the edge of one side. The V_i formed by these points will result in large different sizes of the x and y directions of V_i, and its centroid position will be very close to or even overlap the existing piles, which will eventually result in the ineffective location of pile i. If the centre point is searched from the centre to the surrounding area across the raft, the problem of fragmentation of the remaining points will still exist, and then more discontinuous "leftover material" will be generated. Finally, the centroid of V_i assembled from these corner materials will be invalid.

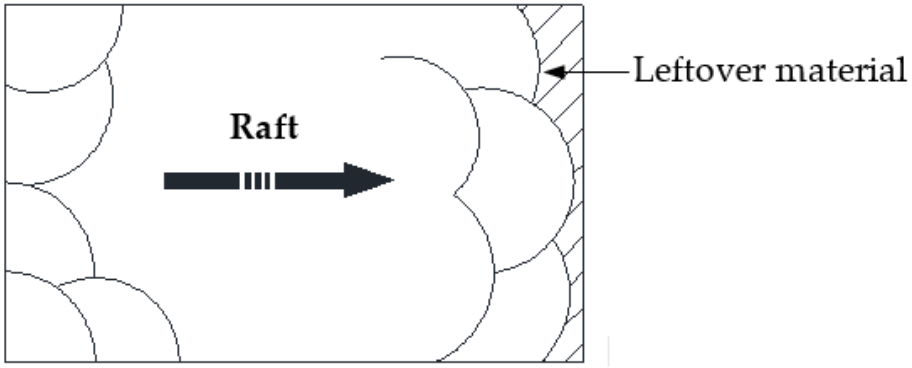


Figure 3. Search central points on the raft from left to right.

Therefore, in order to minimize the error caused by "leftover material", a better way is needed. This paper uses the "cast net" search method (as shown in Figure 4) to solve this problem. We select a fixed point (P_{fix}), and then always select the point farthest from P_{fix} as the central point. As the central points gradually move closer to P_{fix}, all the "leftover materials" are gathered near the P_{fix}, which avoids more dispersed "leftover material" as much as possible. Although the shape distortion of V_N is still unavoidable, the error produced by the "leftover material" is reduced greatly compared with other search methods.

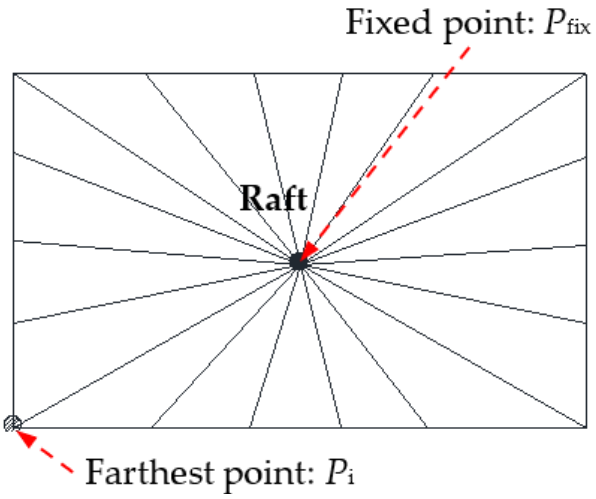


Figure 4. "Cast net" search method.

In theory, P_{fix} can be any point on the raft. However, the V_N, where P_{fix} is located, is a gathering place of "leftover material"; the shape will be twisted inevitably, resulting in a large error of the last pile's position. In order to reduce the influence of this error, the last pile should not be the corner pile or side pile. P_{fix} should be far from the corner and edge of

the raft as much as possible. The research [18,29] shows that a P_{fix} close to the centre of the raft or the location of the maximum settlement of the raft (if it is not at the edge or corner of the raft) can be selected to share the errors caused by the distortion of the V_N shape.

V_T is a volume consisting of many discrete blocks, which cannot be evenly divided into N groups, and there will inevitably be errors. When $V_i \geq V_{avg}$ is chosen as the demarcation line, $V_N \leq V_{avg}$ is an inevitable existence. The effective way to reduce this error is to use as many nodes as possible to discretize the settlement surface.

3.3. Find the Centroid of V_i

V_i corresponding to pile i is expressed using the discrete function as follows:

$$V_i = \sum_{j=1}^{N_i} (Z_j \times a_0) \tag{5}$$

where N_i is the total number of point P_i and its sub-points. Z_j is the settlement of point j, which can be found in $[Z]$ according to the co-ordinates of point j.

The x and y co-ordinates of each node associated with V_i and the corresponding settlement z can be extracted during the use of CSM, and then the centroid formula of the volume can be used:

$$x_{ic} = \frac{\sum_{j=1}^{N_i} v_j \times X_j}{V_i} = \frac{\sum_{j=1}^{N_i} Z_j \times a_0 \times X_j}{\sum_{j=1}^{N_i} Z_j \times a_0} = \frac{\sum_{j=1}^{N_i} Z_j \times X_j}{\sum_{j=1}^{N_i} Z_j} \tag{6}$$

$$y_{ic} = \frac{\sum_{j=1}^{N_i} v_j \times Y_j}{V_i} = \frac{\sum_{j=1}^{N_i} Z_j \times a_0 \times Y_j}{\sum_{j=1}^{N_i} Z_j \times a_0} = \frac{\sum_{j=1}^{N_i} Z_j \times Y_j}{\sum_{j=1}^{N_i} Z_j} \tag{7}$$

where X_j and Y_j are the co-ordinates of point j in matrices $[X]$ and $[Y]$; Equations (6) and (7) are expressed in matrix form as follows:

$$x_{ic} = \frac{[X_j][Z_j]^T}{\sum_{j=1}^{N_i} Z_j} \tag{8}$$

$$y_{ic} = \frac{[Y_j][Z_j]^T}{\sum_{j=1}^{N_i} Z_j} \tag{9}$$

Finally, (x_{ic}, y_{ic}) is the location of the pile i.

3.4. Optimal Iteration

If the influence of the pile–soil interaction is neglected, the differential settlement can be eliminated theoretically after optimization design. However, the pile–soil interaction after optimization is not the same as before optimization because of the change in pile arrangement. Therefore, a differential settlement will inevitably exist. In order to achieve better optimization efficiency, an optimal iteration is needed. The information of the nodes at the top of the raft is extracted from the calculation results of the optimization scheme, and the raft settlement surface is interpolated using the same interpolation points as in the initial design. The generated $[X]$ and $[Y]$ matrices are the same as the original design, while $[Z]$ (raft settlement) is different, expressed as $[Z]_m$. $Z_{\min}$ is the minimum value in $[Z]_m$, and

lets each element in $[Z]_m$ minus $Z_{\min}$ form a new matrix $[Z]_m'$, which can be called the differential settlement matrix. The differential settlement matrix $[Z]_m'$ is superposed to $[Z]$, which was used previously, to form a new raft settlement surface as follows:

$$[Z]_{i+1} = [Z]_m' + [Z]_i \tag{10}$$

Then, the new $[Z]_{i+1}$ is used to re-optimize the design, where i represents the number of cycles. This cycle lasts until the optimization rate meets the requirement.

3.5. Objective Function and Design Constraints

In this study, the objective function of the AOM can be expressed as:

$$\text{Minimize} \quad \Delta S = S_{max} - S_{min} \tag{11}$$

where S_{max} and S_{min} are the maximum and minimum settlements of the raft, respectively. ΔS is the differential settlement of the raft.

Based on the design guidelines for a large pile group in the China code [30] and the general design practice [14,31], several design constraints are imposed on the optimization foundation:

(1) Constraint 1: During the optimization process, the minimum pile spacing is no smaller than twice the pile diameter to satisfy the constructability and structural requirements [12,14,32]; otherwise, stop the optimization loop. Therefore, this paper suggests that the pile spacing should be no less than thrice the pile diameter in the initial design.

(2) Constraint 2: The maximum load (P_{max}) on top of the piles after optimization design is no higher than its ultimate bearing capacity (UBC) (P_u). Otherwise, increase the number of piles and recalculate this iteration until $P_{max} \leq P_u$.

(3) Constraint 3: The differential settlement can only be reduced indefinitely and cannot be eliminated entirely because of the influence of the pile–soil interaction. Therefore, it is necessary to set an upper limit on the objective function to terminate the optimization loop. While the increment ($\Delta F_{m+1} = F_{m+1} - F_m$) of the optimization rate (F) of the differential settlement is smaller than 5%, stop the optimization; m represents the number of iterations; F is the optimization rate and defined as:

$$F = \frac{R - R'}{R} \tag{12}$$

where R and R' are the results from the initial design and the optimized design, respectively. The results can be the settlement of the raft and the stress on top of the piles.

The flow chart of AOM is shown in Figure 5.

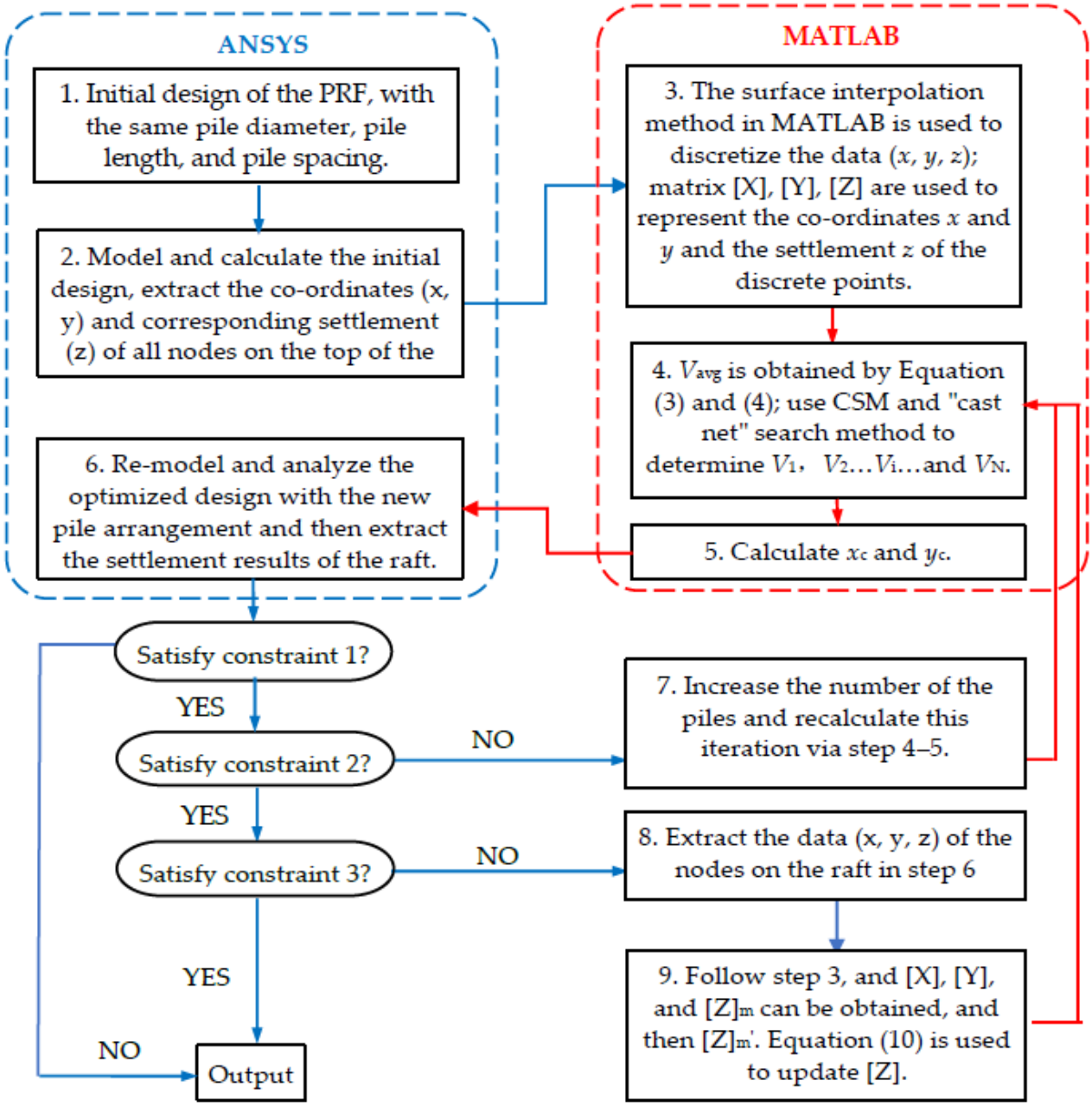


Figure 5. Flowchart of AOM.

4. Illustrative Example

4.1. PRF Model and Material

The initial designs of the PRFs used in this paper are designed by the traditional design method ("identical" piles with the same length, pile diameter, and constant pile spacing). Both of the PRFs in Case 1 and Case 2 consist of 117 concrete piles arranged in a 9 × 13 pattern and connected with a raft (40 m × 58 m) with a thickness of 1.8 m. The only difference is that the load in Case 1 is a uniform load and in Case 2 is a non-uniform load. Case 3 consists of 211 concrete piles and is connected with an irregular raft (see Figure 6) with the same thickness of 1.8 m, and the load is a non-uniform load. The length (37 m) and diameter (1.5 m) of the piles in the three models are the same, and the length and diameter are located with approximately the same center-to-center spacing equal to 3 diameters. In order to reduce the effect of boundary conditions, the sizes of the PRFs in the horizontal direction are approximately 3~4 times greater than the raft size; the detailed dimensions are shown in Figure 7. The detailed material parameters of the raft, pile, and bedrock are listed

in Table 1. The ground of the models contains the same soils, which has seven soil layers and one bedrock layer; the detailed parameters are reported in Table 2. The solid element is used to model the soil and piled raft foundations. Considering the influence of pile–soil interaction, the soil around the pile is adopted with a more precise unit size than other soil to show the difference between the deformation characteristics of the soil around the pile and other soil. As a result, the maximum element sizes in the vertical and horizontal direction are 0.7 m and 6 m, respectively. There are about 2.4×10^5–4×10^5 nodes and 3.9×10^5–6.4×10^5 elements.

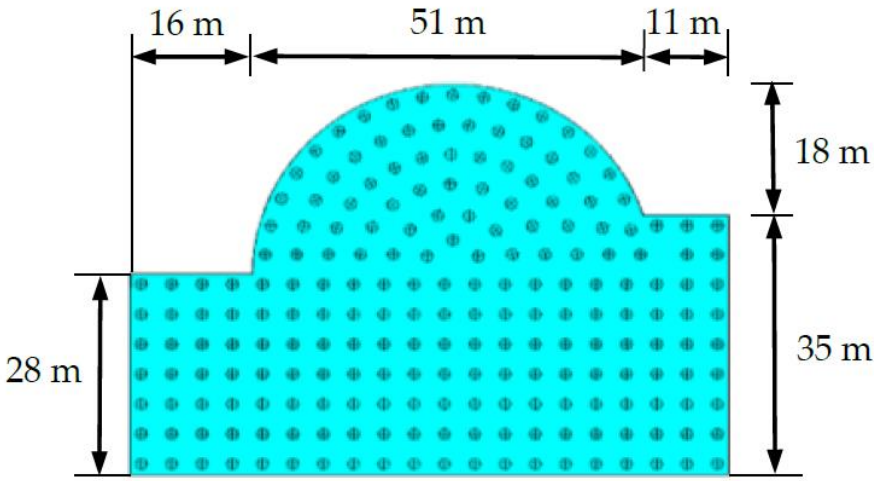
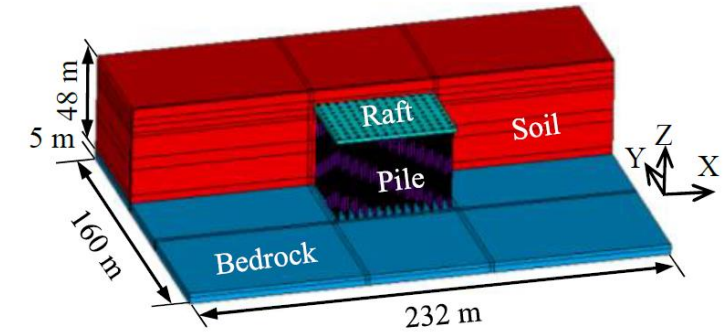
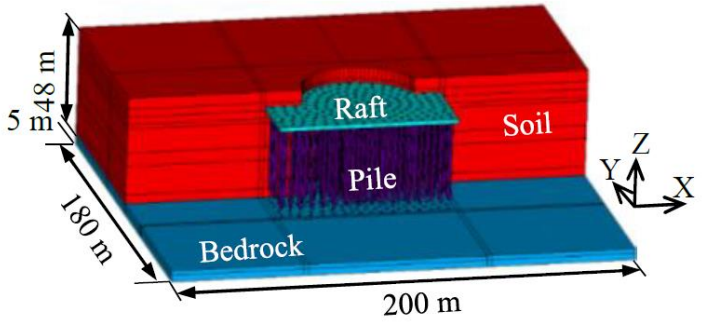


Figure 6. Detailed dimensions of the irregular raft in Case 3.

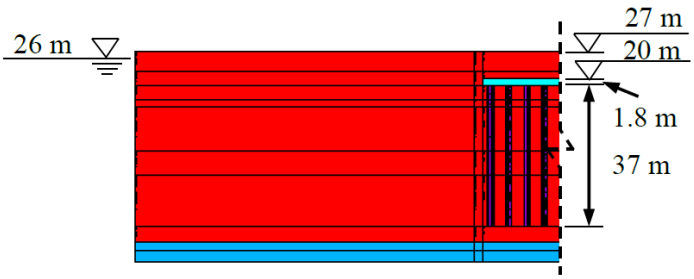


(**a**)



(**b**)

Figure 7. *Cont.*



(**c**)

Figure 7. Different view of PRFs: (**a**) the model of Case 1 and Case 2; (**b**) the model of Case 3; (**c**) cross-section view of the models of three cases.

Table 1. Parameters of raft, pile, and bedrock.

Property	Elastic Modulus (Pa)	Poisson's Ratio	Density (kg/m^3)
Pile	3×10^{10}	0.2	2.4×10^3
Raft	2×10^{10}	0.2	2.4×10^3
Bedrock	1.5×10^{10}	0.3	2.5×10^3

Table 2. Soil parameters of the Duncan–Chang (DC) model used in this paper [29].

Soil Type	High-Level (m)	R_f	k	n	G	F	D	k_{ur}	φ (°)	c (kPa)	ρ_s (g/cm^3)
Fine sand	18.4~27.4	0.9	642	0.6	0.4	0	0	972	37.1	15	1.1
Fine sand	15.5~18.4	0.8	672	0.6	0.4	0	0	1009	38.2	16	1.1
Medium-coarse gravel	13.5~15.5	0.8	519	0.55	0.4	0	0	781	34.9	12	1.2
Medium-coarse sand	1.9~13.5	0.7	462	0.5	0.4	0	0	701	34.6	11	1.1
Medium-coarse gravel	−3.9~1.9	0.8	502	0.6	0.4	0	0	762	38.1	16	1.2
Fine sand	−16.9~−3.9	0.9	431	0.6	0.4	0	0	663	34.6	16	1.1
Medium-coarse gravel	−21~−16.9	0.8	568	0.6	0.4	0	0	901	34.2	20	1.1

In this paper, the Duncan–Chang (DC) model [33,34] used in this paper is an incremental nonlinear (hyperbolic) stress-dependent model, in which the tangent modulus and Poisson's ratio are expressed in an incremental relationship, and the relationship between strain and stress is nonlinear. During the analysis, the initial principal stress (σ_1 and σ_3) of the soil is obtained through a finite element calculation, and then the initial elastic modulus of the soil can be obtained by inputting it into the DC constitutive model, and then the external load is gradually applied. After the calculation of each load step, the three principal stresses of each soil element are output, and then the adjusted soil elastic modulus and Poisson's ratio are obtained from the DC model and used as the soil parameters for the next calculation. Equation (13) is used to obtain σ_1 and σ_3, where z is the distance from the ground to the center of soil element, γ is the gravity per unit volume of the soil, and K_0 is the static lateral pressure coefficient.

$$\begin{cases} \sigma_1 = \gamma z \\ \sigma_3 = K_0 \gamma z \end{cases} \quad \text{where, } K_0 = 0.95 - \sin\varphi \tag{13}$$

4.2. Load and Boundary Conditions

In the model, the loads on the raft are all applied to the nodes on the top surface of the raft, and the loads are all divided into 20 steps to consider the non-linear characteristics of soil layers during the construction. The shape of the surface loads in different models are shown in Figure 8. The first load step (i = 1) of the three cases are all the gravity of the soil layers, and the other 19 load steps have the same load shape and value (total load/19) in Case 1 and Case 2, while that in Case 3 are different; see Figure 8 and Table 3, where P

represents the total load distribution of raft plane. A rigid boundary condition was used at the bottom of the model, i.e., all the nodes with a Z co-ordinate of −26 m are constrained in three directions. The peripheral nodes around the model only have displacement in the Z direction, and the motion in the X and Y directions is constrained.

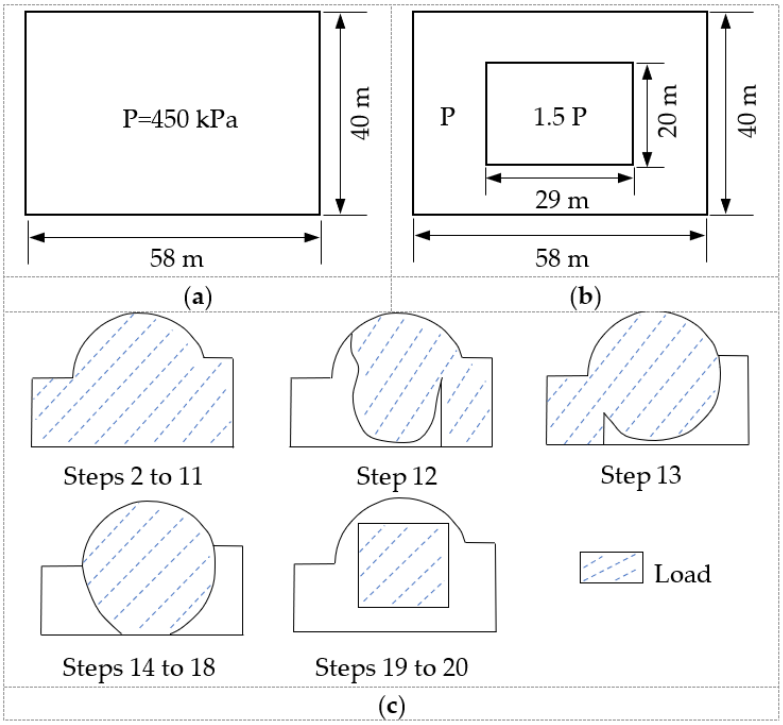


Figure 8. The shape of surface loads in different cases: (**a**) uniform load in Case 1; (**b**) non-uniform load in Case 2; (**c**) the load shape of each step in Case 3.

Table 3. The value of each load step in Case 3.

Step	1	2	3	4	5	6	7	8	9	10	11	12	13	14	15	16	17	18	19	20
Load (MN)	-	86	209	67	119	44	68	75	1	108	27	38	27	6	32	48	3	25	38	77

5. Results by AOM

5.1. Different Pile Arrangement

The optimization design of the PRFs in Case 1 and Case 2 converge after two iterations, and in Case 3 after three iterations. Figure 9 shows the initial pile arrangement in each case together with the optimal pile arrangement determined by each final iteration. The range of the pile spacing after optimization design in Case 1 is 3.7 m to 5 m, in Case 2, it is 3.0 m to 5.3 m, and in Case 3 is 3.1 m to 5.6 m. The results show that whether the load is uniform or non-uniform, more piles are placed around the centre of the raft after optimization design, which agrees with Randolph's argument [35]. These arrangements are due to two factors: (1) the load at the raft center is too large, and (2) the raft center is the place where the pile–soil interaction in the pile group is repeatedly superimposed, which will also cause its settlement to be greater than that of other areas of the raft. The larger loads are in the centre of the raft and the influence of the pile–soil interaction on the centre piles, which are larger than on the surrounding piles.

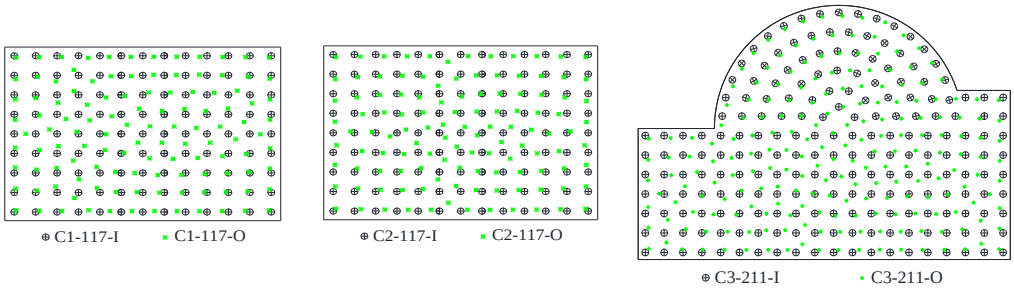


Figure 9. Pile arrangements of different models: (**a**) initial design (C1-117-I) and optimization design (C1-117-O) of Case 1; (**b**) initial design (C2-117-I) and optimization design (C2-117-O) of Case 2; (**c**) initial design (C3-211-I) and optimization design (C3-211-O) of Case 3.

5.2. Settlements of the Raft

Figure 10 gives the 3 D views of the raft settlement in different models. Comparison results show that the differential settlements of the rafts in different cases are all considerably reduced with the optimal pile arrangements, and the rafts settle nearly as a rigid body. The detailed data is shown in Table 4; the maximum settlements of the raft are all reduced compared with that in initial designs due to reasonable pile arrangements, which indicates that the stiffness of the PRFs in each case is improved. The minimum settlements of the raft are all increased after optimization design, which means the utilization rate of the bearing capacity of the piles are more than those in the initial design. The differential settlement of the raft for Case 1 is changed from 0.011 m to 0.0018 m with F = 83%, while that for Case 2 is reduced from 0.024 m to 0.0022 m with F = 91%, and that for Case 3 is changed from 0.023 m to 0.0021 m with F = 91%. The high optimization rates of different models indicate that the AOM has high robustness, which is affected slightly by the load type and the raft shape.

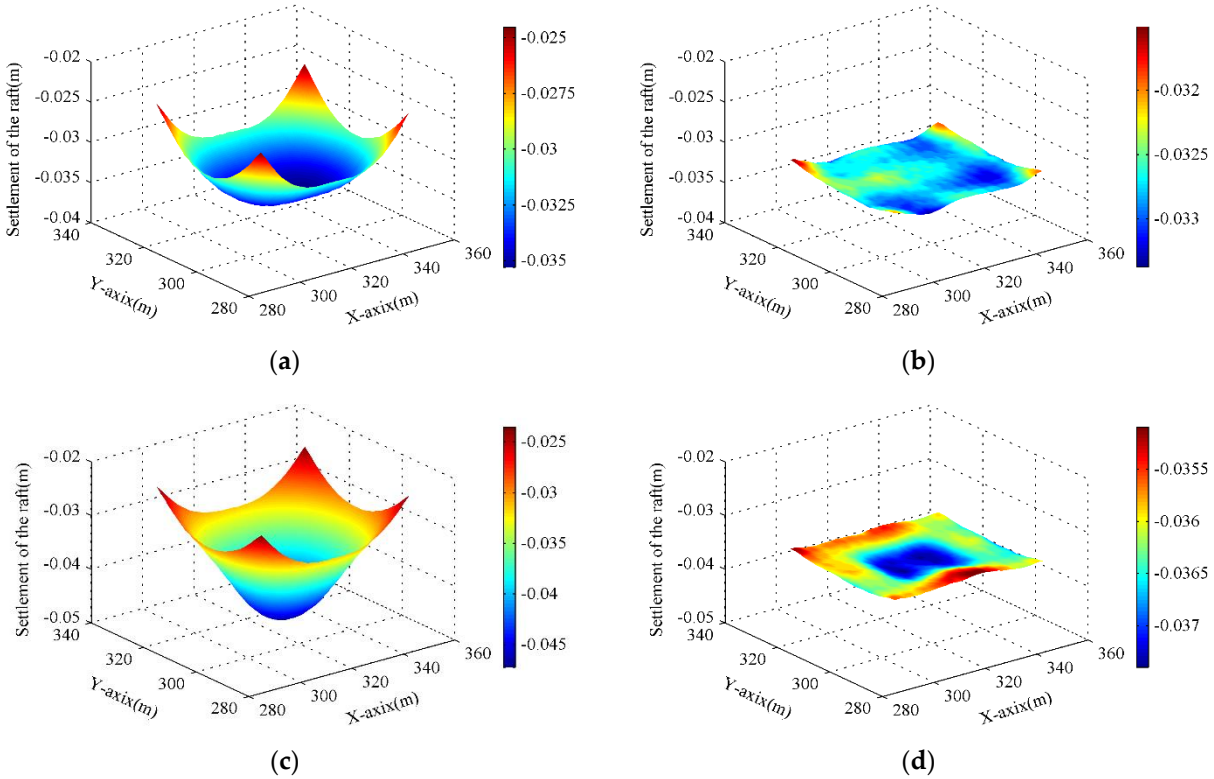
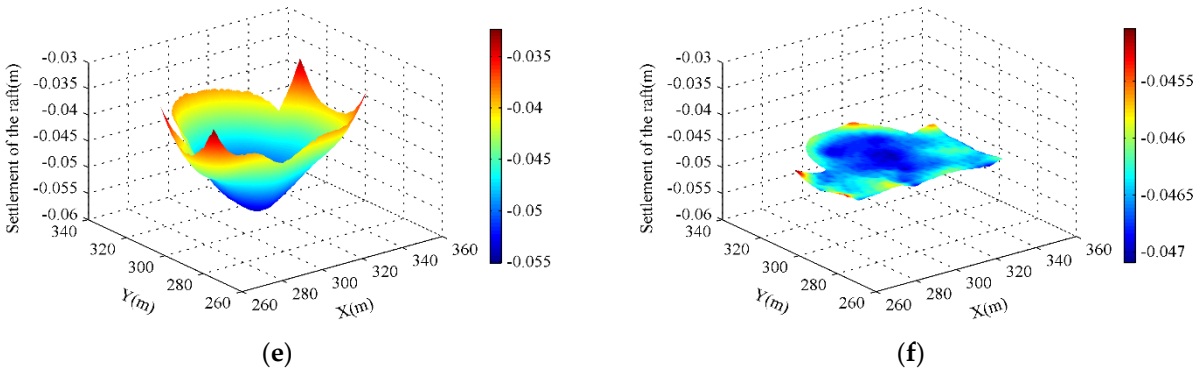


Figure 10. *Cont.*



(**e**) (**f**)

Figure 10. Settlements of the raft in different cases before and after optimization design: (**a**) C1-117-I; (**b**) C1-117-O; (**c**) C2-117-I; (**d**) C2-117-O; (**e**) C3-211-I; (**f**) C3-211-O.

Table 4. Comparison of settlements of the rafts for different cases (m).

Model	C1-117-I	C1-117-O	C2-117-I	C2-117-O	C3-211-I	C3-211-O
Min-S	0.024	0.0315	0.023	0.035	0.032	0.045
Max-S	0.035	0.0333	0.047	0.037	0.055	0.047
Diff-S (*F*)	0.011	0.0018	0.024	0.0022	0.023	0.0021
	-	(83%)	-	(91%)	-	(91%)

Note: "Min" is short for Minimum; "Max" is short for Maximum; "Diff" is short for differential; "-S" is short for settlement.

5.3. Stresses on Top of Piles

The pile length, pile diameter, and the soil layers of the PRFs used in this paper are the same as that in XIE and CHI [29]. Therefore, the UBC of the piles is 17.2 MN (the related stress on top of the pile is 9.7 MPa), and the introduction of the relevant calculation method and verification is no longer repeated here. The comparison of the pile top stress and corresponding UBC can reflect the utilization ratio of the bearing capacity of the pile. Table 5 shows that the minimum pile top stresses of different cases are all increased, which means the optimization design used more bearing capacity compared with the initial design, and without the pile top stress exceeding the UBC.

Table 5. Comparison of stresses on top of the piles among different schemes (MPa).

Model	C1-117-I	C1-117-O	C2-117-I	C2-117-O	C3-211-I	C3-211-O
Min-Stress	3.13	3.24	3.15	3.53	4.7	5.8
Max-Stress	3.68	3.91	5.22	4.3	7.95	6.52
Diff-Stress	0.55	0.67	2.07	0.77	3.25	0.72
UBC	9.7	9.7	9.7	9.7	9.7	9.7

Note: "Min" is short for Minimum; "Max" is short for Maximum; "Diff" is short for differential.

Differential stress refers to the difference value between the minimum and maximum stress on top of the pile group; it is affected by the pile soil interaction (PPI) and/or non-uniform load, and the influence mechanisms are different between them. The differential stress of the pile group in Case 1 is increased by 22%, while it is decreased by 63% in Case 2 and 78% in Case 3 after optimization design. The reason is that the main differential stress in Case 1 is only due to the PPI while the other two cases have one more reason: non-uniform load. The effects from PPI will always exist when the PPI always exists, and therefore the corresponding differential stress cannot be removed completely. In this view, the AOM is more suitable for PRF with the non-uniform load. However, the reduction of the differential settlement (in Table 4) is the most important optimization target in this paper; as long as the maximum pile top stress does not exceed the UBC, the increase of differential stress on top of the pile group is not considered temporary.

6. Reduction in the Cost of the Pile Group

6.1. Translation of the Excess Bearing Capacity of the Piles into Economic Savings

As is shown in Table 5, the maximum pile top stresses are all below the UBC after optimization design, which means the piles still have excess bearing capacity (EBC). This part tries to translate EBC into the reduction of the cost of the pile group. In order to keep enough safety stock for the pile groups, some constraints are given as follows:

(1) Max-Stress at the pile top is below the UBC whether before or after the optimization design;
(2) After the optimization design, the maximum pile top stress of the pile group shall not be greater than the initial design calculation result or half of the ultimate bearing capacity of a single pile bearing capacity (short for (1/2)UBC), which is commonly used in the Chinese code [31].

During this process, it is assumed that the load is only taken by piles:

$$P_{total} = \sum_{i=1}^{N} P_i = \sum_{i=1}^{N} \sigma_i A_P \tag{14}$$

where P_{total} is the load on top of the raft, P_i is the load supported by pile i, N is the number of piles in the initial design, and A_P is the area of the pile section (piles have the same diameter in this study). It is assumed that the pile groups can get into an ideal working state, which means the bearing capacity of each pile is equally utilized after optimization design. In this way, the stress on top of each pile is almost the same, that is:

$$\sigma_1 = \ldots \sigma_i = \ldots \sigma_N \tag{15}$$

Then, Equation (14) can be expressed as

$$P_{total} = N\sigma_i A_P = N_{new}\sigma_{i,new} A_P \text{ , where } N_{new} = (1 - F_{extra})N \tag{16}$$

N_{new} and $\sigma_{i,new}$ are the new number of piles and the new pile top stress of the new final optimization scheme. According to Equation (16), N can be reduced by the same percent as the increment (F_{extra}) of stress (σ_i) to a target stress (σ_{target}) to keep P_{total} unchanged. σ_{target} is an upper limit of the pile top stress from the new optimization scheme, which should take the maximum value between the maximum pile top stress in the initial design and (1/2) UBC (the constraints as mentioned before). The F_{extra} is expressed as:

$$F_{extra} = \frac{\sigma_{target} - \sigma_{max,o}}{\sigma_{target}} \tag{17}$$

where $\sigma_{max,o}$ is the maximum pile top stress of the pile group after optimization design by AOM. F_{extra} is assumed as the EBC of a pile group. The EBC is translated to the reduction of the number of piles, which is also equal to the reduction of the total cost for the pile group. In order to reduce the number of iterations, optimization design in this part can be continued based on the optimization result by AOM, and the settlement matrix [Z] is updated using the result of the optimized model. N is changed to N_{new} during the re-using of AOM during this process.

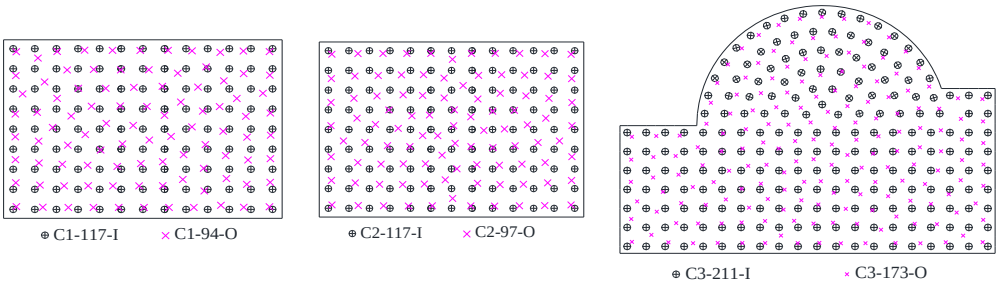
6.2. Results after Optimization Design Considering Economic Saving (AOM-ES)

The optimization process of PRF for Case 1 converges after two iterations based on C1-117-O, and that for Case 2 converges after one iteration based on C2-117-O, while that for Case 3 converges after three iterations based on C3-211-O. The final number of piles after AOM-ES in each case and the corresponding parameters are listed in Table 6. Figure 11 presents the pile arrangements of the three cases after AOM-ES together with those in the initial design. The distribution characteristic of the pile spacing is similar to that in Figure 9; for instance, more piles are placed around the centre of the raft. For fewer piles compared

with that in the initial design, the pile spacing of the pile group increases obviously. The range of the pile spacing after AOM-ES in Case 1 is 3.7 m to 5.5 m, in Case 2 3.3 m to 5.7 m, and in Case 3 3.5 m to 5.9 m.

Table 6. Comparison of the three cases during AOM-ES.

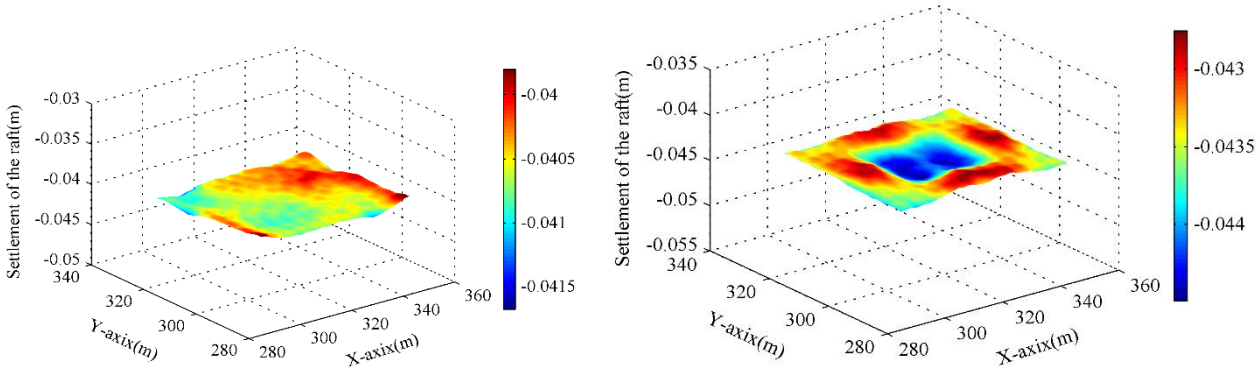
Model	C1-117-I	C2-117-I	C3-211-I
σ_{target} (MPa)	4.85	5.22	7.95
$\sigma_{max,o}$ (MPa)	3.91	4.3	6.52
F_{extra}	19%	17%	18%
N_{new}	94	97	173



(**a**) (**b**) (**c**)

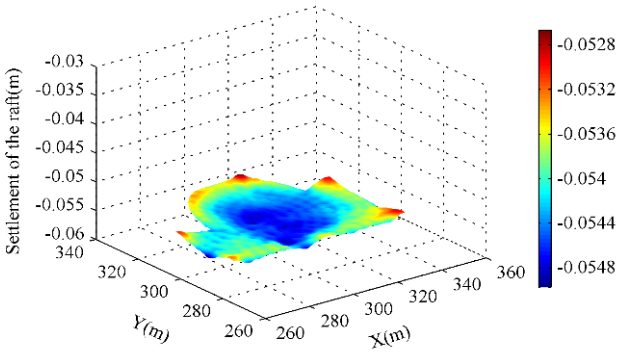
Figure 11. Pile arrangements of initial designs and AOM-ES: (**a**) initial design and AOM-ES (C1-94-O) of Case 1; (**b**) initial design and AOM-ES (C2-97-O) of Case 2; (**c**) initial design and AOM-ES (C3-173-O) of Case 3.

Compared with Figure 11a,c,e, Figure 12 presents the 3 D view of the raft settlements in each case after AOM-ES, which shows that the raft settlements are more uniform than that in the initial design. Table 7 gives the detailed comparison of the corresponding data. The minimum and maximum settlements of the raft in the three cases are all increased, which are affected by the reduction of the number of piles, while these increases did not affect the decrease of the differential settlements (the optimization rates are still no less than 80%). For the same reason, fewer piles are used in the models after AOM-ES, and the minimum and maximum pile top stresses are all increased, which indicates that the bearing capacity of the piles are more utilized than that in the initial design and first optimization design (by AOM), without pile top stress excess in the corresponding UBC.



(**a**) (**b**)

Figure 12. *Cont.*



(**c**)

Figure 12. Raft settlements of the three cases after optimization design: (**a**) C1-94-O; (**b**) C2-97-O; (**c**) C3-173-O.

Table 7. Comparison of settlements of the rafts and pile top stress for different cases after AOM-ES.

Model	Min-S (m)	Max-S (m)	Diff-S (m) (*F*)	Min-Stress (MPa)	Max-Stress (MPa)	Diff-Stress (MPa)	UBC
C1-94-O	0.0398	0.0417	0.0019 (82%)	3.96	4.57	0.61	9.7
C2-97-O	0.0428	0.0445	0.0018 (92%)	4.19	4.92	0.73	9.7
C3-173-O	0.0526	0.055	0.0024 (90%)	7.07	7.77	0.7	9.7

Note: "Min" is short for Minimum; "Max" is short for Maximum; "-S" is short for settlement; "Diff" is short for differential.

As mentioned in the previous part, the bearing capacity of the soil is neglected. However, the load shared by the soil actually increases as the number of piles reduces. Therefore, the load shared by the piles in models after AOM-ES is always less than that in the optimization design only by AOM, as follows:

$$N\sigma_i A_P \geq N_{new}\sigma_{i,new} A_P \tag{18}$$

As a result, $\sigma_{i,new}$ will not exceed σ_{target} because of the existence of the soil and the influence of the pile–soil interaction. Finally, the volume of the pile group in C1-94-O is reduced by 19%, in C2-97-O by 17%, and in C3-173-O by 18% compared with the initial design, which means the costs of the pile groups are reduced by the same percent without sacrificing too many bearing capacity stock of the pile group.

7. Conclusions

An adaptive optimization method is developed for the pile arrangement of a piled raft foundation in this paper. In the method, the pile spacing is adjusted according to the settlement of the raft from an initial design (designed by the traditional design method). Pile groups subjected to uniform and non-uniform loads and different shapes of the rafts use the proposed optimization algorithm via the finite element method. During this process, the soil inhomogeneity and nonlinearity are also considered. According to the research results, the following conclusions are drawn:

1. Without increasing the consumption of total pile material, varying the pile spacing across the pile group can affect the overall foundation behaviour, as the maximum settlements of the raft in three cases are reduced compared with that in the initial design. The optimization rates of the differential settlement of the raft are all more than 80%, and only need few iterations during the optimization process. The minimum pile top stresses are increased in three cases, which indicates that more bearing capacity is utilized after optimization design compared with the initial design. The compared

results indicate that the AOM method proposed in this paper has high optimization efficiency and robustness.

2. For the case where the maximum bearing capacity of the piles after optimization design is less than that in the initial design or does not exceed the design value in the code (1/2 UBC), an economic optimization design of the piled raft foundation under certain safety conditions can be achieved by reducing the number of piles. The results show that no pile top stress from different PRFs exceeds the UBC after optimization design, and the bearing capacity of the piles with minimum pile top stress are all more utilized than that in the initial design. The reduction of the number of piles does not affect the differential stress on top of the pile group significantly compared with those in optimization designs only by AOM, and the optimization rates of the differential settlement of the raft are still more than 80%. These benefits can not only be translated into economic savings but also reduce the environmental impacts, as less construction materials will be consumed.
3. The lower limit of pile spacing during the optimization process is a problem requiring engineering judgment. Twice the pile diameter as the low limit of the pile spacing in this paper is a suggestion based on existing experience, and it can be adjusted according to construction technology and engineering requirements. On the other hand, in order to reduce the limitation of the lower limit of pile spacing on the optimization efficiency (constraint 1), piles as long as possible (with larger pile spacing) can be selected under a given load during the initial design to ensure sufficient optimization space to achieve a higher optimization rate.

Author Contributions: Conceptualization, methodology, software, validation, formal analysis, investigation, data curation, writing original draft, C.Y.; supervision, writing—review and editing, Y.X.; supervision, writing—review and editing, methodology, M.O. All authors have read and agreed to the published version of the manuscript.

Funding: We are grateful for the support and the help of Key Research and Development and Promotion Project in Henan Province (Grant No. 212102310269), Open Research Fund of Key Laboratory of Construction and Safety of Water Engineering of the Ministry of Water Resources, China Institute of Water Resources and Hydropower Research (Grant No.202110), and Scientific Research Project of North China University of Water Resources and Electric Power (Grant No. 201811007, No.202104009), Open Research Fund of Key Laboratory of Construction and Safety of Water Engineering of the Ministry of Water Resources, China Institute of Water Resources and Hydropower Research (Grant No.202110).

Institutional Review Board Statement: Not applicable.

Informed Consent Statement: Not applicable.

Data Availability Statement: Data underlying the results presented in this paper are not publicly available at this time but may be obtained from the authors upon reasonable request.

Acknowledgments: We are grateful for the support and the help of Jason Jonkman for providing the FAST code.

Conflicts of Interest: The authors declare no conflict of interest.

References

1. Eslami, A.; Malekshah, S.S. Analysis of non-connected piled raft foundations (NCPRF) with cushion by finite element method. *Comput. Methods Civ. Eng.* **2011**, *2*, 153–168.
2. Basile, F. Non-linear analysis of vertically loaded piled rafts. *Comput. Geotech.* **2015**, *63*, 73–82. [CrossRef]
3. Sinha, A.; Hanna, A. 3D Numerical Model for Piled Raft Foundation. *Int. J. Geomech.* **2017**, *17*, 04016055. [CrossRef]
4. Ravichandran, N.; Shrestha, S.; Piratla, K. Robust design and optimization procedure for piled-raft foundation to support tall wind turbine in clay and sand. *Soils Found.* **2018**, *58*, 744–755. [CrossRef]
5. Patil, G.; Choudhury, D.; Mondal, A. Three-dimensional soil-foundation-superstructure interaction analysis of nuclear building supported by combined piled-raft system. *Int. J. Geomech.* **2021**, *21*, 04021029. [CrossRef]

6. Mohamad, Z.; Fardoun, F.; Meftah, F. A review on energy piles design, evaluation, and optimization. *J. Clean. Prod.* **2021**, *292*, 125802. [CrossRef]
7. Bhaduri, A.; Choudhury, D. Serviceability-based finite-element approach on analyzing combined pile-raft foundation. *Int. J. Geomech.* **2020**, *20*, 04019178. [CrossRef]
8. Bourgeois, E.; Hassen, G.; Buhan, P.D. Finite element simulations of the behavior of piled-raft foundations using a multiphase model. *Int. J. Numer. Anal. Methods Geomech.* **2013**, *37*, 1122–1139. [CrossRef]
9. Nguyen, V.T.; Hassen, G.; Hassen, P. A multiphase approach for evaluating the horizontal and rocking impedances of pile group foundations. *Int. J. Numer. Anal. Methods Geomech.* **2016**, *40*, 1454–1471. [CrossRef]
10. Kelly, R.; Huang, J.; Poulos, H.; Stewart, M.G. Geotechnical and structural stochastic analysis of piled solar farm foundations. *Comput. Geotech.* **2021**, *132*, 103988. [CrossRef]
11. Kim, K.N.; Lee, S.H.; Kim, K.S.; Chung, C.K.; Kim, M.M.; Lee, H.S. Optimal pile arrangement for minimizing differential settlements in piled raft foundations. *Comput. Geotech.* **2001**, *28*, 235–253. [CrossRef]
12. Hurd, A.J.; Truman, K.Z. Optimization method of pile foundations. In Proceedings of the Advances in Engineering Structures, Mechanics & Construction, Waterloo, ON, Canada, 14–17 May 2006; pp. 653–661.
13. Chan, C.M.; Zhang, L.M.; Ng, J.T. Optimization of pile groups using hybrid genetic algorithms. *J. Geotech. Geoenviron. Eng.* **2009**, *135*, 497–505. [CrossRef]
14. Liang, F.Y.; Chen, L.Z.; Han, J. Integral equation method for analysis of piled rafts with dissimilar piles under vertical loading. *Comput. Geotech.* **2009**, *36*, 419–426. [CrossRef]
15. Liang, F.Y.; Song, Z. BEM analysis of the interaction factor for vertically loaded dissimilar piles in saturated poroelastic soil. *Comput. Geotech.* **2014**, *36*, 223–231. [CrossRef]
16. Nguyen, D.D.C.; Kim, D.S.; Jo, S.B. Settlement of piled rafts with different pile arrangement schemes via centrifuge tests. *J. Geotech. Geoenviron. Eng.* **2013**, *139*, 1690–1698. [CrossRef]
17. Nguyen, D.D.C.; Kim, D.S.; Jo, S.B. Parametric study for optimal design of large piled raft foundations on sand. *Comput. Geotech.* **2014**, *55*, 14–26. [CrossRef]
18. Xie, Y.; Chi, S. Optimization method of reducing the differential settlements of piled raft foundations based on pile-to-pile interaction theory. *Adv. Civ. Eng.* **2020**, *2*, 1–14. [CrossRef]
19. Sanctis, L.D.; Mandolini, A.; Russo, G.; Viggiani, C. Some Remarks on the Optimum Design of Piled Rafts. In Proceedings of the International Deep Foundations Congress, Orlando, FL, USA, 14–16 February 2002; pp. 405–425.
20. Li, Y.; Wang, J.; Wang, Q.; Yang, K. Optimization Design Study on Variable Stiffness of the Pile Raft Foundation in High-Rise Building. *Adv. Mater. Res.* **2011**, *243*, 2498–2502. [CrossRef]
21. Sales, M.M.; Prezzi, M.; Salgado, R.; Choi, Y.S.; Lee, J. Load-settlement behaviour of model pile groups in sand under vertical load. *J. Civ. Eng. Manag.* **2017**, *23*, 1148–1163. [CrossRef]
22. Padfield, C.J.; Sharrock, M. *Settlement of Structures on Clay Soils*; Construction Industry Research & Information Institute: London, UK, 1983.
23. Kim, H.T.; Yoo, H.K.; Kang, I.K. Genetic algorithm-based optimum design of piled raft foundations with model tests. *J. Southeast Asian Geotech. Soc.* **2002**, *33*, 1–11.
24. Leung, Y.F.; Klar, A.; Soga, K.; Hoult, N.A. Superstructure–foundation interaction in multi-objective pile group optimization considering settlement response. *Can. Geotech. J.* **2017**, *54*, 1408–1420. [CrossRef]
25. Shrestha, S.; Ravichandran, N.; Rahbari, P. Geotechnical Design and Design Optimization of a Pile-Raft Foundation for Tall Onshore Wind Turbines in Multilayered Clay. *Int. J. Geomech.* **2017**, *18*, 04017143. [CrossRef]
26. Ng, J.T.M.; Chan, C.M.; Zhang, L.M. Optimum design of pile groups in nonlinear soil using genetic algorithms. In Proceedings of the 8th International Conference on the Application of Artificial Intelligence to Civil, Structural and Environmental Engineering, Rome, Italy, 30 August–2 September 2005; p. 35.
27. Hwang, J.H.; Lyu, Y.D.; Chung, M.C. Optimizing pile group design using a real genetic approach. In Proceedings of the International Offshore and Polar Engineering Conference, Maui, HI, USA, 19–24 June 2011; pp. 491–499.
28. Liu, X.; Cheng, G.; Wang, B.; Lin, S. Optimum design of pile foundation by automatic grouping genetic algorithms. *ISRN Civ. Eng.* **2012**, *2012*, 678329. [CrossRef]
29. Xie, Y.; Chi, S. Optimization Method for Irregular Piled Raft Foundation on Layered Soil Media. *Adv. Civ. Eng.* **2019**, *2019*, 5713492. [CrossRef]
30. *JGJ94*; Technical Code for Building Pile Foundations. Ministry of Housing and Urban-Rural Development of the People's Republic of China: Beijing, China, 2008.
31. Poulos, H.G.; Carter, J.P.; Small, J.C. Foundations and retaining structures-Research and practice. In Proceedings of the 15th International Conference on Soil Mechanics and Geotechnical Engineering, Istanbul, Türkiye, 27–31 August 2001; pp. 2527–2606.
32. Letsios, C.; Lagaros, N.D.; Papadrakakis, M. Optimum design methodologies for pile foundations in London. *Case Stud. Struct. Eng.* **2014**, *2*, 24–32. [CrossRef]
33. Chen, S.P.; Yao, W.J.; Zhu, S.Q. Nonlinear Finite Element Analysis of Super-Long Pile and Soil Interaction in Soft Soil. *Proc. Adv. Mater. Res. Trans. Tech. Publ.* **2011**, *201*, 1601–1605. [CrossRef]

34. Duncan, J.M.; Chang, C.Y. Nonlinear analysis of stress and strain in soils. *J. Soil Mech. Found. Div.* **1970**, *96*, 1629–1653. [CrossRef]
35. Randolph, M.F. Design methods of pile groups and piled rafts. In Proceedings of the 13th International Conference on Soil Mechanics and Foundation Engineering, New Delhi, India, 5–10 January 1994; Volume 5, pp. 61–82.

Disclaimer/Publisher's Note: The statements, opinions and data contained in all publications are solely those of the individual author(s) and contributor(s) and not of MDPI and/or the editor(s). MDPI and/or the editor(s) disclaim responsibility for any injury to people or property resulting from any ideas, methods, instructions or products referred to in the content.